

Quantum critical transition from charge-ordered to superconducting state in the triangular lattice negative- U extended Hubbard model

S. Mazumdar

Department of Physics, University of Arizona Tucson, AZ 85721

R.T. Clay

*Department of Physics and Astronomy and HPC² Center for Computational Sciences,
Mississippi State University, Mississippi State MS 39762*

(Dated: November 10, 2018)

We demonstrate a robust frustration-driven charge-order to superconductivity transition in the half-filled negative- U extended Hubbard model. Superconductivity extends over a broad region of the parameter space. We argue that the model provides the correct insight to understanding unconventional superconductivity in the organic charge-transfer solids and other quarter-filled systems.

PACS numbers: 74.70.Kn, 74.20.-z, 74.20.Mn

Spatial broken symmetries such as antiferromagnetism (AFM) and charge ordering (CO) are proximate to superconductivity (SC) in a number of exotic systems, including the cuprates¹, $\text{Na}_x\text{CoO}_2 \cdot y\text{H}_2\text{O}$ ², $\beta\text{-Na}_{0.33}\text{V}_2\text{O}_5$ ³ and organic charge-transfer solids (CTS) such as $(\text{TMTCF})_2\text{X}$ (here $\text{C}=\text{S}$ or Se , and X are closed-shell anions)⁴, $(\text{BEDT-TTF})_2\text{X}$ (hereafter ET_2X)⁴ and $\text{EtMe}_3\text{Z}[\text{Pd}(\text{dmit})_2]_2$, $\text{Z} = \text{P}, \text{As}$ ⁵. Unlike in the cuprates, SC in the CTS is reached not by doping, but on application of hydrostatic or uniaxial pressure. CTS crystals often consist of anisotropic triangular lattices of dimers of the active cationic or anionic molecules. The average number of charge carriers n per molecule is $\frac{1}{2}$, indicating that n per dimer unit cell is 1. Since the $n = 1$ triangular lattice provides the classic template for the resonating valence bond (RVB) electronic structure within the nearest-neighbor (n.n.) Heisenberg Hamiltonian⁶, the idea that spin frustration drives an AFM-to-SC or spin liquid-to-SC transition in the CTS has acquired popularity⁷. Within this picture, pressure makes the effective anisotropic $n = 1$ triangular lattice more isotropic, and SC occurs over a narrow range of anisotropy between the more robust AFM and the paramagnetic metal (PM). Numerical quantum Monte Carlo⁸ and exact diagonalization⁹ calculations, however, have failed to find superconducting correlations in the the triangular lattice repulsive $n = 1$ Hubbard model, casting doubt on the mean-field techniques that find SC within the Hamiltonian. Experimentally, the situation is complex. (i) SC in certain CTS is proximate to CO instead of AFM¹⁰. This has led to yet other mean-field models with additional Coulomb parameter of charge-fluctuation mediated SC¹¹. (ii) The insulating phase proximate to SC in $\text{EtMe}_3[\text{Pd}(\text{dmit})_2]_2$ is not an AFM but a valence bond solid (VBS), with *charge disproportionation* between molecules¹². (iii) AFM is missing in the insulating state of $\kappa\text{-ET}_2\text{Cu}_2(\text{CN})_3$ with a nearly isotropic triangular lattice¹³. There occur inhomogeneous charge localization and sharp decrease in spin susceptibility below 10 K¹⁴, which may also be signatures of a static or fluctuat-

ing VBS-like state. Whether or not frustration can drive transition to SC from an ordered state therefore remains an open and intriguing question.

In the present paper we demonstrate a robust frustration-driven SC within the $n = 1$ negative- U extended Hubbard model (EHM) with n.n. Coulomb repulsion V . Although the literature on the negative- U Hubbard Hamiltonian is vast, the model has been investigated primarily for bipartite lattices. With repulsive V , there is strong tendency to CO in bipartite lattices and SC is absent¹⁵. Frustrated lattices have been investigated within the Hamiltonian for $V = 0$ only¹⁶. Now SC dominates and CO is absent. Here we begin with the square lattice with n.n. V and electron hopping, when the ground state is a checkerboard CO with alternate double occupancies and vacancies in the square lattice. As the Coulomb interaction and electron hopping along one diagonal of the square lattice increase from zero, charge frustration in the emergent triangular lattice leads to first-order transition to a superconducting state. While our primary goal is to demonstrate the frustration-driven CO-to-SC transition, we also point out that our work provides insight for understanding unconventional SC in $n = \frac{1}{2}$ correlated electron systems including the CTS.

We consider the two-dimensional (2D) Hamiltonian,

$$H = -t \sum_{\langle ij \rangle, \sigma} (c_{i, \sigma}^\dagger c_{j, \sigma} + H.c.) - t' \sum_{[kl], \sigma} (c_{k, \sigma}^\dagger c_{l, \sigma} + H.c.) - |U| \sum_i n_{i, \uparrow} n_{i, \downarrow} + V \sum_{\langle ij \rangle} n_i n_j + V' \sum_{[kl]} n_k n_l \quad (1)$$

on an anisotropic triangular lattice. Here $c_{i, \sigma}^\dagger$ creates an electron with spin σ (\uparrow, \downarrow) on site i , $n_{i, \sigma} = c_{i, \sigma}^\dagger c_{i, \sigma}$, and $n_i = \sum_\sigma n_{i, \sigma}$. U is the on-site Hubbard interaction; $\langle \dots \rangle$ implies n.n. along the x- and y-axes, with hopping integral and Coulomb repulsion t and V , respectively. Similarly, $[\dots]$ implies neighbors along the (x+y)-diagonal, with t' and V' as the hopping and Coulomb integrals. We have chosen the same signs for t and t' , as the results

for $n = 1$ are independent of the relative sign of t' . In the following we express all quantities in units of t . For simplicity we consider mostly $V' = V$, although we have performed calculations also for other V' . Nonzero V' and t' are both crucial for the CO-to-SC transition.

We have performed exact diagonalizations on a 16-site periodic lattice. The quantities we calculate are the structure factor $S(\vec{Q})$, the bond-order B_d along the $(x + y)$ -diagonal, and the pair correlation function $P(r)$, which are defined as,

$$S(\vec{Q}) = \frac{1}{N} \sum_{j, \vec{r}} \exp(i\vec{Q} \cdot \vec{r}) \langle (n_j - 1)(n_{j+\vec{r}} - 1) \rangle \quad (2a)$$

$$B_d = \sum_{\sigma} \langle c_{j, \sigma}^{\dagger} c_{j+\hat{x}+\hat{y}} + H.c. \rangle \quad (2b)$$

$$P(r) = \frac{1}{N} \sum_j \langle c_{j, \uparrow}^{\dagger} c_{j, \downarrow}^{\dagger} c_{j+\vec{r}, \downarrow} c_{j+\vec{r}, \uparrow} \rangle \quad (2c)$$

We begin with the numerical results for $U = -2$ and $V = V' = 1$, for which a first-order like CO-to-SC transition occurs in our finite lattice at $t'_c = 0.5$. In Figs. 1(a) and (b) we have plotted $S(\vec{Q})$ versus \vec{Q} for $t' = 0.45$ and $t' = 0.5$, respectively. The sharp peak at $\vec{Q} = (\pi, \pi)$ in Fig. 1(a) is a signature of the checkerboard CO, with doubly occupied and vacant sites alternating along the x and y -directions (see Fig. 4(b)). The amplitude of the CO remains practically unchanged between $t' = 0$ and 0.48 (see below). The complete absence of the $S(\vec{Q})$ peak in Fig. 1(b) indicates a sudden loss of the CO due to the mobility acquired by the electron pairs. The latter in turn leads to superconducting pair correlations, as seen in Fig. 1(c), where we have plotted $P(r)$ against r (where r is in units of the lattice constant) for both $t' = 0.45$ and 0.5. For $r = 1.414$, $P(r)$ has two different values corresponding to diagonals along $x + y$ and $x - y$, respectively. We have chosen to show the smaller of the two, corresponding to the nonbonded sites along $x - y$, in Fig. 1(c). The large increase in $P(r)$ for all r (by more than a factor of 2 at n.n., and nearly an order of magnitude at larger r) as t' changes from 0.45 to 0.5, as well as the weak dependence of $P(r)$ on r beyond $r = 1$ are signatures of a SC ground state for $t' = 0.5$. While SC is present in the model at electron densities $n \neq 1$, the CO-to-SC transition is unique to $n = 1$. Our calculations were done also for $V' \neq V$. The ground state continues to be CO for all t' for $V' = 0$, with the amplitude nearly independent of t' (not shown). Furthermore, $P(r)$ in this case is nearly 0 for all $r > 1$. Thus both nonzero V' and t' are essential for frustration. We have, however, determined that the CO-to-SC transition occurs here at nearly the same t'_c for $V' = t'$.

To illustrate the sharpness of the CO-to-SC transition in this case we have plotted in Fig. 2(a) $S(\pi, \pi)$ and B_d against t' for the same U, V as in Fig. 1. The sudden drop in $S(\pi, \pi)$ and the jump in B_d occur at the same t'_c , indicating that the vanishing of the CO is due to sudden increase in carrier mobility. Fig. 2(b) shows a plot of

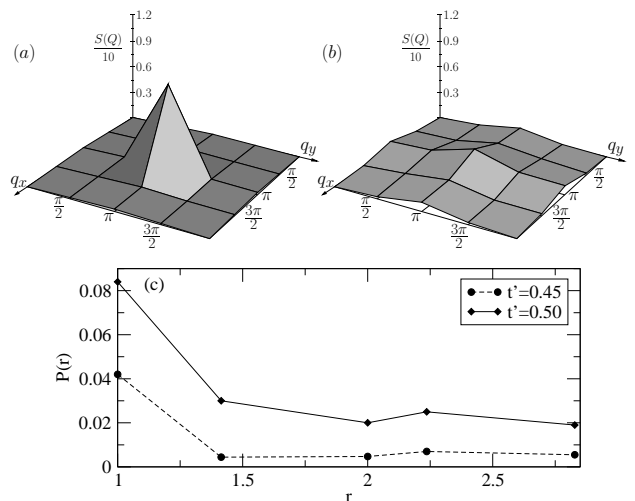


FIG. 1: (a) and (b), $S(\vec{Q})$ vs. \vec{Q} for $U = -2$, $V = V' = 1$ and $t' = 0.45$ and $t' = 0.5$, respectively. (c) $P(r)$ vs. r , for $t' = 0.45$ (dashed curve) and $t' = 0.5$ (solid curve).

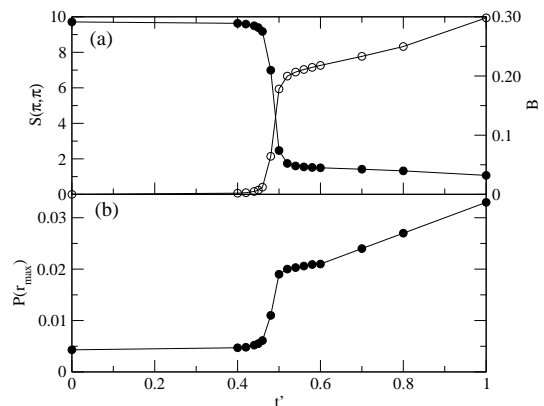


FIG. 2: (a) $S(\pi, \pi)$ (filled circles) and B_d (unfilled circles) vs. t' for $U = -3$, $V = V' = 1$. (b) $P(r_{max})$ vs. t' for the same Coulomb interactions.

$P(r_{max} = 2.428)$, where the jump in the pair-correlation occurs at the same t'_c , indicating that charge mobility is due to pair motion. The results of Fig. 2 indicate that coexistence of CO and SC occurs over a very narrow region of the parameter space, if at all, for this moderately strongly correlated case. This is in contrast to the mixed CO-SC state that is obtained when instead of t' and V' the carrier concentration n is varied¹⁵.

Within Eq. 1, the amplitude of the CO at $t' = 0$ increases with both $|U|$ and V . As might be expected, the stronger the CO in the $t' = 0$ limit, the larger is the t'_c at which the CO-to-SC transition occurs. Furthermore, it is known that for $V = 0$ the CO and SC states are degenerate in the square lattice. It is then to be expected that the transition is second order for weak V , independent of the value of $|U|$. We show a $t' - |U|$ phase diagram for fixed $V = 1$ in Fig. 3(a). The transition remains first order like for this moderate V until $|U|$ is large. Our

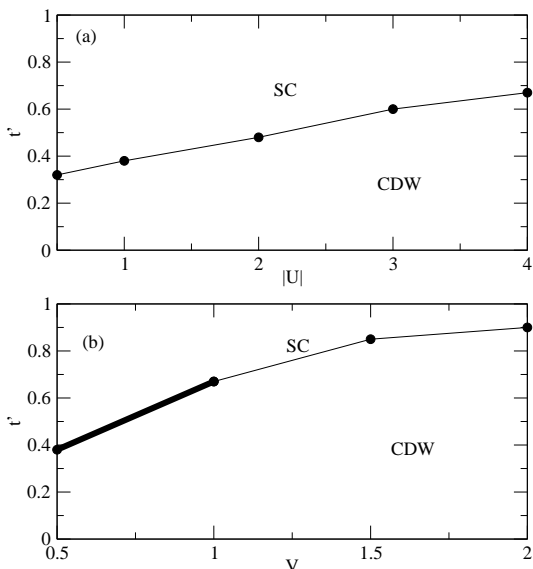


FIG. 3: Phase diagrams of the frustrated EHM at zero temperature in (a) the $t' - |U|$ plane for fixed $V = 1$; (b) the $t' - V$ plane for fixed $U = -4$. The transition is first order (continuous) for large (small) V in (b). The SC phase persists in the $t' > 1$ region until $t' \gg 1$.

phase diagram in the $t' - V$ space in Fig. 3(b) is for fixed $|U| = 4$. Surprisingly, when both $|U|$ and V are large ($|U| = 4$, $V = 2$) the ground state continues to be the checkerboard CO for t' as large as 0.9.

The SC phase within Eq. 1 is robust and occurs over a broad region in the phase diagrams in Figs. 3(a) and (b). For the $|U|$ values of interest SC is lost only for $t' \gg 1$. This is in sharp contrast to the results obtained within the spin frustration model with repulsive U , where even within the approximate methods that claim SC, the bulk of the $t' - U$ parameter space is occupied by AFM and PM phases, and SC occurs as an intermediate phase for a narrow range of t' for each U^7 .

We now speculate how the negative- U EHM in the weak $|U|$ limit may be relevant to the CTS, β - $\text{Na}_{0.33}\text{V}_2\text{O}_5$ and other $n = \frac{1}{2}$ systems. Our fundamental premise is that the behavior of $\text{EtMe}_3\text{Z}[\text{Pd}(\text{dmit})_2]_2$ and $\kappa\text{-ET}_2\text{Cu}_2(\text{CN})_3$ with nearly isotropic lattices is representative of the more anisotropic systems at very low temperatures and under pressure, when V' and t' are large. The mapping of the molecular $n = \frac{1}{2}$ lattice into the effective $n = 1$ repulsive Hubbard Hamiltonian that describes the AFM phase requires *homogeneous* charge population on the dimer unit cells⁷. We postulate that under pressure the AFM phase switches over to a static or fluctuating VBS with *inhomogeneous* charge distribution (see below), and the effective $n = 1$ Hamiltonian that describes this state is different. We rationalize this hypothesis based on our recent work. The complete Hamiltonian for these systems must start from the $n = \frac{1}{2}$ *repulsive- U* EHM. In a series of papers¹⁷, we have established that the ground state of the $n = \frac{1}{2}$ repulsive Hamiltonian is often

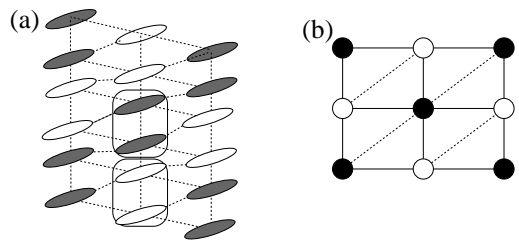


FIG. 4: (a) BCDW corresponding to the VBS in the 2D organic layer. Filled (unfilled) ellipses correspond to charge-rich (charge-poor) molecules. (b) Pairs of charge-rich and charge-poor molecules constitute the double occupancy (filled circle) and vacancy (empty circle) in the effective $n = 1$ lattice.

a Bond-Charge-Density Wave (BCDW), with charge occupancy $\dots 1100 \dots$, where ‘1’ and ‘0’ refer to molecular charges $0.5 + \epsilon$ and $0.5 - \epsilon$, respectively. This is a *quantum* effect driven by the antiferromagnetic correlations due to the repulsive U and dominates over the classical effect due to V that favors the formation of the Wigner crystal $\dots 1010 \dots$ for $V < V_c(U)$, where $V_c(U)$ can be as large as 3 for realistic U^{17} . The BCDW is enhanced by the intersite electron-phonon interactions that modulate the hopping integral, and the intrasite Holstein electron-molecular vibration couplings¹⁷. Most importantly, even when at high temperatures there occurs a Wigner crystal CO in the $(\text{TMTTF})_2\text{X}$, the low temperature spin-Peierls phase is the BCDW¹⁷. We postulate that the $\dots 1100 \dots$ is a *bipolaron density wave* that can be modeled by an *effective $n = 1$* negative- U EHM, where the effective sites are alternating pairs of occupied (1-1) and unoccupied (0-0) molecules, respectively. That the sites of a negative- U EHM for a complex system can be composite ones has been suggested previously¹⁵. Note that the traditional mapping of $n = \frac{1}{2}$ into effective $n = 1$ AFM⁷ also assumes composite dimer sites, with the only difference that our proposed mapping is valid for the inhomogeneous charge distribution.

The $\dots 1100 \dots$ charge occupancy persists for dimensionality greater than 1¹⁸. Experimentally, the 2D BCDW has been seen in the weakly 2D $(\text{TMTSF})_2\text{X}$, the triangular lattice $\theta\text{-ET}_2\text{X}$, the ladder materials $(\text{DTTTF})_2\text{M}(\text{mnt})_2$ ($\text{M}=\text{Au}, \text{Cu}$), and $\text{EtMe}_3[\text{Pd}(\text{dmit})_2]_2$. The co-existing $2k_F$ charge- and spin-density waves¹⁹ in $(\text{TMTSF})_2\text{X}$ has been explained as a Bond-Charge-Spin Density Wave²⁰. The experimentally observed horizontal charge stripe in the $\alpha\text{-ET}_2\text{X}$ and $\theta\text{-ET}_2\text{X}$ consists of $\dots 1100 \dots$ charge occupancies occurring along the two directions of strong hoppings¹⁸. The large spin gap in the two-chain $(\text{DTTTF})_2\text{M}(\text{mnt})_2$ ²¹ can be understood within the $n = \frac{1}{2}$ zigzag ladder model²², within which there occur interchain singlets and the $\dots 1100 \dots$ charge occupancy along the zigzag diagonals²². We point out that

charge occupancies and the bonding patterns in the VBS $\text{EtMe}_3\text{P}[\text{Pd}(\text{dmit})_2]_2$ (see Fig. 3(b) in Ref. 12 and Fig. 4) correspond precisely to the $\cdots 1100 \cdots$ BCDW. Finally, $\beta\text{-Na}_{0.33}\text{V}_2\text{O}_5$ consists of $n = \frac{1}{2}$ V chains and ladders, and there is extensive literature on n.n. intersite bipolarons in this and related systems²³ (the earlier literature did not emphasize the $n = \frac{1}{2}$ carrier concentration that is crucial for the mapping into the effective $n = 1$ Hamiltonian).

We therefore postulate that $n = \frac{1}{2}$ systems at low temperatures and under pressure can be understood qualitatively within the effective $n = 1$ negative- U EHM. This “mapping” is seen in Fig. 4, where we have shown the intersite bipolaron CDW corresponding to the VBS in $\text{EtMe}_3\text{P}[\text{Pd}(\text{dmit})_2]_2$ ¹², as well as the corresponding $n = 1$ checkerboard CO. We speculate that for small t' within the $n = \frac{1}{2}$ molecular system, the occupancies of the dimer unit cells are indeed homogeneous, which gives the AFM in this region. The larger t' or lattice distortion (or both) at low temperatures give the insulating VBS with CO, and at still larger t' the intersite spin singlets become mobile, which is approximately modeled in our calculations within the effective negative- U EHM. We emphasize that intersite (as opposed to intrasite) bipolarons have been shown to be light and mobile, *especially in the triangular lattice*²⁴, and will be even more so here

as the binding is due to antiferromagnetic correlations and not overscreening of V by electron-phonon interactions. Finally, although SC within the effective Hamiltonian is s -wave, this need not be true within the actual $n = \frac{1}{2}$ repulsive- U EHM with intersite pairs.

In summary, we have shown that it is indeed possible to have frustration-driven SC, within a model that emphasizes charge as opposed to spin-correlations. We have also suggested that the $n = \frac{1}{2}$ VBS insulator can be conceived as an effective $n = 1$ bipolaron CDW. A complete theory of SC in the CTS should of course demonstrate the CO-to-SC transition within the actual $n = \frac{1}{2}$ repulsive- U EHM with electron-phonon interactions, but we believe that our work on the effective $n = 1$ Hamiltonian gives the insight necessary for constructing such a theory. In particular, the approach opens up the possibility of describing all CTS as well as inorganic $n = \frac{1}{2}$ systems within one simple model. An interesting aspect of our work is that the configuration space pairing in the VBS, and by implication in the superconducting state within the present model occurs due to a co-operative interaction between AFM correlations and electron-phonon interactions, and thus SC mediated by these two interactions need not be mutually exclusive.

This work was supported by the Department of Energy grant DE-FG02-06ER46315.

-
- ¹ J. G. Bednorz and K. A. Müller, Z. Phys. B **64**, 189 (1986).
² K. Takada et al., Nature **422**, 53 (2003).
³ T. Yamauchi, Y. Ueda, and N. Mori, Phys. Rev. Lett. **89**, 057002 (2002).
⁴ T. Ishiguro, K. Yamaji, and G. Saito, *Organic Superconductors* (Springer-Verlag, New York, 1998).
⁵ R. Kato et al., J. Am. Chem. Soc. **128**, 10016 (2006).
⁶ P. W. Anderson, Mater. Res. Bull. **8**, 153 (1973).
⁷ K. Miyagawa and K. Kanoda, Chem. Rev. **104**, 5635 (2004); B. J. Powell and R. H. McKenzie, J. Phys. Condens. Matter **18**, R827 (2006); J. Schmalian, Phys. Rev. Lett. **81**, 4232 (1998); K. Kuroki and H. Aoki, Phys. Rev. B **60**, 3060 (1999); M. Vojta and E. Dagotto, Phys. Rev. B **59**, R713 (1999); G. Baskaran, Phys. Rev. Lett. **90**, 197007 (2003); J.Y. Gan et al., Phys. Rev. Lett. **94**, 067005 (2005); B. Kyung and A.-M. S. Tremblay, Phys. Rev. Lett. **97**, 046402 (2006); T. Watanabe et al., J. Phys. Soc. Jpn. **75**, 074707 (2007).
⁸ T. Mizusaki and M. Imada, Phys. Rev. B **74**, 014421 (2006).
⁹ H. Li, S. Mazumdar, and R. T. Clay, in preparation.
¹⁰ N. Tajima et al., J. Phys. Soc. Jpn. **71**, 1832 (2002); A. F. Bangura et al., Phys. Rev. B **72**, 014543 (2005); H. Nishikawa et al., Phys. Rev. B **72**, 052510 (2005).
¹¹ J. Merino and R. H. McKenzie, Phys. Rev. Lett. **87**, 237002 (2001).
¹² M. Tamura, A. Nakao, and R. Kato, J. Phys. Soc. Jpn. **75**, 093701 (2006).
¹³ Y. Shimizu et al., Phys. Rev. Lett. **91**, 107001 (2003).
¹⁴ A. Kawamoto and Y. Honma and K. Kumagai, Phys. Rev. B **70**, 060510 (R) (2004); A. Kawamoto et al., Phys. Rev. B **74** 212508 (2006).
¹⁵ R. Micnas, J. Ranninger, and S. Robaskiewicz, Rev. Mod. Phys. **62**, 113 (1990).
¹⁶ R. R. dos Santos, Phys. Rev. B **48**, 3976 (1993); C. Chen, Phys. Rev. B **48**, 6683 (1993); T. Nakano and K. Kuroki, Phys. Rev. B **74**, 174502 (2006).
¹⁷ K. C. Ung, S. Mazumdar, and D. Toussaint, Phys. Rev. Lett. **73**, 2603 (1994); R. T. Clay, S. Mazumdar, and D. K. Campbell, Phys. Rev. B **67**, 115121 (2003); R. T. Clay, R. P. Hardikar, and S. Mazumdar, Phys. Rev. B **76**, 205118 (2007).
¹⁸ S. Mazumdar, R. T. Clay, and D. K. Campbell, Phys. Rev. B **62**, 13400 (2000); R. T. Clay, S. Mazumdar, and D. K. Campbell, J. Phys. Soc. Jpn. **71**, 1816 (2002).
¹⁹ J. P. Pouget and S. Ravy, Synth. Metals **85**, 1523 (1997).
²⁰ S. Mazumdar et al., Phys. Rev. Lett. **82**, 1522 (1999).
²¹ X. Ribas et al., Adv. Funct. Mater. **15**, 1023 (2005).
²² R. T. Clay and S. Mazumdar, Phys. Rev. Lett. **94**, 207206 (2005); J. L. Musfeldt et al., to appear in Solid State Sci.
²³ B. K. Chakraverty, M. J. Sienko, and J. Bonnerot, Phys. Rev. B **17**, 3781 (1978).
²⁴ J. Bonca and S. A. Trugman, Phys. Rev. B **64**, 094507 (2001); H. Fehske, J. Loos and G. Wellein, *ibid* **61**, 8016 (2000); J. P. Hague et al., Phys. Rev. Lett. **98**, 037002 (2007).